Supporting information for: *Ab initio* Characterization of the Electrochemical Stability and Solvation Properties of Condensed-Phase Ethylene Carbonate and Dimethyl Carbonate Mixtures

Taylor A. Barnes,[†] Jakub Kaminski,[‡] Oleg Borodin,[¶] and Thomas F. Miller III[*,†]

Division of Chemistry and Chemical Engineering, California Institute of Technology, Pasadena, CA 91125 , Department of Mathematics, University of California, Los Angeles, CA 90095 , and U.S. Army Research Laboratory, Electrochemistry Branch, Sensors & Electron Devices Directorate, 2800 Powder Mill Road, Adelphi, MD 20783

E-mail: tfm@caltech.edu

[*]To whom correspondence should be addressed

[†]Division of Chemistry and Chemical Engineering, California Institute of Technology, Pasadena, CA 91125

[‡]Department of Mathematics, University of California, Los Angeles, CA 90095

[¶]U.S. Army Research Laboratory, Electrochemistry Branch, Sensors & Electron Devices Directorate, 2800 Powder Mill Road, Adelphi, MD 20783

1 Benchmarking the Electronic Relaxation Calculations

Figure 1 demonstrates both the convergence and accuracy of the electronic relaxation protocol described in Section 2.3.2 of the main text. Results are provided for the errors, relative to full B3LYP calculations, of a series of IEs calculated using supermolecular ($r_{\text{border}} = \infty$) B3LYP-in-B3LYP/cc-pVDZ embedding. Inclusion of the electronic relaxation energy is observed to reduce the errors by approximately an order of magnitude, with a single iteration of the third step of the electronic relaxation protocol being sufficient to converge the energies. As a result, all relaxation calculations in the main text are performed using a single iteration of the relaxation protocol.

The data are calculated for twelve geometry configurations, obtained by modifying a single configuration from the EC ensemble. Each configuration includes the molecule in the active region and one of the molecules in the DFT region, with the molecule in the active region being replaced by a calcium atom at its center-of-mass, and with the active region corresponding to the calcium atom. This replacement was performed because the low IE of calcium ensures that the electron hole of the oxidized system is well localized on subsystem A, even at the B3LYP level of theory. If this analysis were performed using EC dimers instead of the calcium-EC system, it would be difficult to isolate errors caused by over-delocalization of the B3LYP electron hole (see Section 3.1 of the main text) from errors in the relaxation energy.

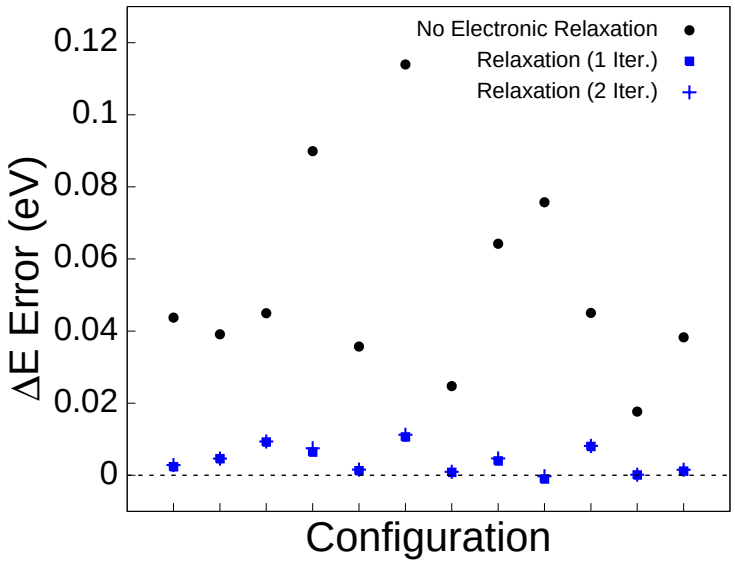

Figure 1: Demonstration of the accuracy of the electronic relaxation protocol described in Section 2.3.2 of the main text. Errors in the vertical IEs of a series of supermolecular B3LYP-in-B3LYP/cc-pVDZ embedding calculations are reported relative to the corresponding full B3LYP calculations. The calculations are performed for the case in which the electronic density of subsystem B is not permitted to relax with respect to the oxidation of subsystem A (black, circles), the case in which the electronic density of subsystem B is permitted to relax in a single iteration (blue, squares), and the case in which the electronic density of subsystem B is permitted to relax in two iterations (blue, pluses).

2 Robustness of the Results with Respect to the Representation of the MM Region

In Section 3.3.3 of the main text, we observed that implicit solvent models substantially underestimate the reorganization energy of DMC, due to the neglect of important quadrupolar interactions. In this section, we demonstrate that this conclusion is robust with respect to the point-charge representation of the MM region.

Table 1 provides the average magnitudes of the molecular dipole and quadrupole moments of both EC and DMC. These results are obtained using B3LYP-in-B3LYP-in-MM/cc-pVDZ embedding on 16 configurations of the neat EC system and 16 configurations of the neat DMC system, taken at 500 ps intervals. The embedding cutoffs are set to $r_{\text{border}} = 0.0$ Å, $r_{\text{DFT}} = 4.0$ Å, and $r_{\text{MM}} = 50.0$ Å. The dipole and quadrupole moments of the molecule in the active region ($\vec{\mathbf{D}}$ and $\overleftrightarrow{\mathbf{Q}}$, respectively) are calculated relative to its center-of-mass, and the magnitudes of these moments are obtained using the expressions $D \equiv \left(\vec{\mathbf{D}} \cdot \vec{\mathbf{D}}\right)^{1/2}$ and $Q \equiv \left(\frac{2}{3}\overleftrightarrow{\mathbf{Q}} : \overleftrightarrow{\mathbf{Q}}\right)^{1/2}$, respectively.[137,138]

Table 1: Magnitude of the Dipole and Quadrupole Moments of EC and DMC

Molecule	$\langle D \rangle_{\text{DFT}}$	$\langle Q \rangle_{\text{DFT}}$	$\langle D \rangle_{\text{MM}}$	$\langle Q \rangle_{\text{MM}}$
EC	6.5(1)	3.2(1)	6.55(3)	3.2(1)
DMC	0.75(5)	11.8(1)	0.56(7)	29.4(1)

The average magnitude of the dipole and quadrupole moments of EC and DMC is obtained using both B3LYP-in-B3LYP-in-MM embedding (DFT), and using the point charge (MM) model described in Section 2.3.3 of the main text. The dipole moments are reported in Debye, while the quadrupole moments are reported in Debye $\cdot$ Å. The value in parentheses indicates the statistical uncertainty in the last reported digit.

Table 1 also provides the average magnitudes of the molecular dipole and quadrupole moments of EC and DMC, obtained using the MM point-charge representation described in Section 2.3.3 of the main text. The molecular dipoles produced by the MM representation accurately reflect those obtained at the DFT level of theory, as expected due to the way in which the point charges were determined in Section 2.3.3 of the main text. For EC, the magnitudes of the B3LYP-level and MM

quadrupoles agree very well, but for DMC, the MM representation overestimates the quadrupole moment by a factor of 2.487. We now investigate this issue to confirm that it does not impact our conclusions from Section 3.3.3.

We first confirm that the reported conclusions regarding the oxidation potential and reorganization energy of neat DMC calculated at the CCSD(T)-in-B3LYP-in-MM level are not sensitive to the magnitude of the quadrupoles in the MM region. In order to examine the sensitivity of the reorganization energy and oxidation potential of neat DMC to the magnitude of the DMC quadrupoles, we perform another set of CCSD(T)-in-B3LYP-in-MM/aug-cc-pVTZ embedding calculations on DMC in both the DMC and DMC^+ systems. This set of calculations utilizes a point-charge representation in which the charge for each atom in the MM region is reduced by a factor of 2.487 relative to the values reported in Table 3 of the main text, and the embedding cutoffs are set to $r_{\text{border}} = 2.5$ Å, $r_{\text{DFT}} = 4.0$ Å, and $r_{\text{MM}} = 50.0$ Å. The resulting value of $\langle \Delta E \rangle_0$ is 10.28 eV, while the value of $\langle \Delta E \rangle_{+1}$ is 8.34 eV. Using these average vertical IEs and Eq. (3) in the main text results in an oxidation potential of 7.91 V vs Li^+/Li. While this value is 0.37 V higher than that reported in Table 5 of the main text, this difference does not affect the conclusion that the oxidation potential of neat EC is higher than that of neat DMC. Similarly, using the above ensemble-averaged vertical IEs and Eq. (1) in the main text results in a solvent reorganization energy of 0.97 eV. The close agreement between this value and the neat DMC reorganization energy of 1.17 eV reported in Table 5 of the main text indicates that our CCSD(T)-in-B3LYP-in-MM reorganization energies are robust with respect to the point-charge representation of the MM region. The somewhat better robustness of the reorganization energies with respect to the parameterization of the point charges is largely a consequence of cancelation of errors in Eq. (1) in the main text.

Secondly, we reconfirm the conclusion from Section 3.3.3 of the main text that quadrupolar intermolecular interactions are important for correctly describing DMC solvation, even if the magnitude of these quadrupolar interactions is reduced by a factor of 2.487. For a series of configurations for the EC^+ system, Figure 2(a) shows $\Delta E_{\text{n}_{\text{th}}\text{-pole}}$, which we define as the contribution of the n_{th} order terms in the multipole expansion of $\Delta E_{\text{n-pole}}$; $\Delta E_{\text{n}_{\text{th}}\text{-pole}}$ results for both the dipole and

quadrupole interactions are plotted. As was observed in Section 4 in the main text, the quadrupolar interactions (blue, squares) in neat EC are negligible compared to the dipolar interactions (black, circles). By contrast, Figure 2(b) demonstrates that the quadrupolar interactions in neat DMC, calculated using the point charges from Section 2.3.3 of the main text, are approximately as large as the corresponding dipolar interactions. Even when the magnitudes of the quadrupole moments in neat DMC are reduced by a factor of 2.487, the resulting quadrupolar interactions (red, triangles) remain comparable to the dipolar interactions. We thus conclude that for any reasonable parameterization of the point charge representation of the MM region, the solvation properties of DMC will be strongly affected by quadrupolar interactions.

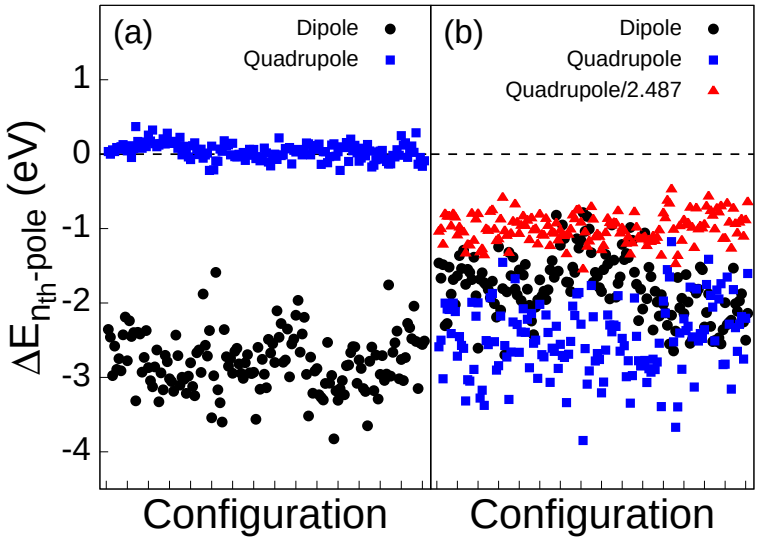

Figure 2: Demonstration that the conclusion that DMC quadrupolar interactions are significant is robust with respect to the parameterization of point charges. (a) The dipolar (black, circles) and quadrupolar (blue, squares) contributions to $\Delta E_{\text{n-pole}}$, $\Delta E_{\text{n}_{\text{th}}\text{-pole}}$, for each configuration of EC^+. (b) As (a), except that the dipolar and quadrupolar contributions are calculated for configurations of DMC^+. Also provided is the contribution of the DMC quadrupoles when the quadrupoles are reduced by a factor of 2.487 (red, triangles).